FISEVIER

Contents lists available at ScienceDirect

Fungal Genetics and Biology

journal homepage: www.elsevier.com/locate/yfgbi



Regular Articles

A metabolomics-guided approach to discover *Fusarium graminearum* metabolites after removal of a repressive histone modification



Donovon A. Adpressa^{a,1}, Lanelle R. Connolly^{b,1}, Zachary M. Konkel^a, George F. Neuhaus^a, Xiao L. Chang^b, Brett R. Pierce^b, Kristina M. Smith^c, Michael Freitag^{b,*}, Sandra Loesgen^{a,*}

- ^a Department of Chemistry, Oregon State University, Corvallis, OR, USA
- ^b Department of Biochemistry and Biophysics, Oregon State University, Corvallis, OR, USA
- ^c Department of Biology, Oregon State University Cascades, Bend, OR, USA

ARTICLE INFO

Keywords: Secondary metabolites Histone methyltransferase Fungi Metabolomics H3K27

ABSTRACT

Many secondary metabolites are produced by biosynthetic gene clusters (BGCs) that are repressed during standard growth conditions, which complicates the discovery of novel bioactive compounds. In the genus Fusarium, many BGCs reside in chromatin enriched for trimethylated histone 3 lysine 27 (H3K27me3), a modification correlated with transcriptional gene silencing. Here we report on our progress in assigning metabolites to genes by using a strain lacking the H3K27 methyltransferase, Kmt6. To guide isolation efforts, we coupled genetics to multivariate analysis of liquid chromatography-mass spectrometry (LCMS) data from both wild type and kmt6, which allowed identification of compounds previously unknown from F. graminearum. We found low molecular weight, amino acid-derived metabolites (N-ethyl anthranilic acid, N-phenethylacetamide, N-acetyltryptamine). We identified one new compound, protofusarin, as derived from fusarin biosynthesis. Similarly, we isolated large amounts of fusaristatin A, gibepyrone A, and fusarpyrones A and B, simply by using the kmt6 mutant, instead of having to optimize growth media. To increase the abundance of metabolites underrepresented in wild type, we generated kmt6 fus1 double mutants and discovered tricinolone and tricinolonoic acid, two new sesquiterpenes belonging to the tricindiol class. Our approach allows rapid visualization and analyses of the genetically induced changes in metabolite production, and discovery of new molecules by a combination of chemical and genetic dereplication. Of 22 fungal metabolites identified here, 10 compounds had not been reported from F. graminearum before. We show that activating silent metabolic pathways by mutation of a repressive chromatin modification enzyme can result in the discovery of new chemistry even in a well-studied organism, and helps to connect new or known small molecules to the BGCs responsible for their production.

1. Introduction

For nearly a century, filamentous fungi have been exploited for their bioactive, industrially important, and agriculturally relevant secondary metabolites (SecMets). Recent genome mining efforts suggested that the capability of fungi to produce SecMets has been severely underestimated (Brakhage, 2013). The majority of SecMet, or biosynthetic, gene clusters (BGCs) are transcriptionally silent under common laboratory culture conditions, prompting the demand for new methods to de-repress these biosynthetic pathways. Reversible post-translational modifications of core histones play essential roles in the regulation of fungal development by changing chromatin structure, and can affect

the regulating of SecMet production (Bok and Keller, 2004; Calvo et al., 2002; Connolly et al., 2013; Fox and Howlett, 2008; Jeon et al., 2015). Perturbing normal histone modifications by chemical or genetic means has been used as a tool to explore the cryptic secondary metabolome but also improves understanding of SecMet function in fungal development (Aghcheh and Kubicek, 2015; Brakhage and Schroeckh, 2011; Cherblanc et al., 2013; Williams et al., 2008).

Earlier studies focused on altering the distribution of histone marks correlated with transcriptionally active regions (e.g., H3K9 acetylation or H3K4me2), a mark for constitutive gene silencing (H3K9me3), a global regulator of secondary metabolism, LaeA, or transcription factors that control carbon and nitrogen metabolism or pH regulation (reviewed in

^{*} Corresponding authors at: Department of Biochemistry and Biophysics, Oregon State University, Corvallis, OR 97331, USA (M. Freitag). Department of Chemistry, Oregon State University, Corvallis, OR 97331, USA (S. Loesgen).

E-mail addresses: Michael.Freitag@oregonstate.edu (M. Freitag), sandra.loesgen@oregonstate.edu (S. Loesgen).

 $^{^{1}}$ Equal contribution.

(Brakhage, 2013). Interfering with histone modifications by use of inhibitors or deleting genes that encode the modifying enzymes can alter the production of bioactive metabolites when compared to wild-type strains (Albright et al., 2015; Bok and Keller, 2004; Connolly et al., 2013; Henke et al., 2016; Jamieson et al., 2013; Niehaus et al., 2013; Sarikaya-Bayram et al., 2014; Smith et al., 2008; Williams et al., 2008).

Previous studies largely focused on enzymes that are required for the expression of BGCs and thus required for the production of SecMets (Albright, 2015; Bok and Keller, 2004; Henke, 2016; Niehaus, 2013; Sarikaya-Bayram, 2014; Williams, 2008). More useful would be mutants in which removal of a global repressor of gene expression results in overexpression of BGCs. We discovered that in F. graminearum the repressive H3K27me3 modification is required for the maintenance of cell identity and the regulation of development, just as in animals and plants (Margueron and Reinberg, 2011; Shaver et al., 2010), and that it also transcriptionally represses numerous BGCs (Connolly et al., 2013; Jamieson et al., 2013; Smith et al., 2008). Thus, removal of H3K27me3 by deletion of the gene (KMT6) for the catalytic subunit, Kmt6, of the Polycomb Repressive Complex 2 (PRC2) resulted in de-repression of ~20% of all genes, including many within known BGCs. More recently, F. fujikuroi strains in which KMT6 was downregulated by an RNAi-mediated approach also allowed identification of novel compounds, yet deletion mutants were not constructed because KMT6 is an essential gene in this species (Studt et al., 2016).

Here we report on our continuing efforts to assign known and previously unknown *F. graminearum* metabolites to genes or BGCs. Except for carotenoids, we previously did not explicitly show that increased transcriptional activity -and thus elevated RNA levels- directly correlates with overproduction of SecMets (Connolly et al., 2013). By a combination of medium throughput metabolomics and genetic dereplication, we have identified 22 of 44 metabolites significantly overproduced in the *kmt6* mutant on rich medium. This includes a dozen compounds previously known from this species but also 10 metabolites not previously reported from *F. graminearum*, though many had been described before from other fungi. Three compounds are new, demonstrating that this method may help to find new compounds, even though *F. graminearum* has been extensively studied over the past decades.

2. Materials and methods

2.1. Strains and culture conditions

A wild-type (WT) *F. graminearum* strain (PH-1) and the *kmt6* deletion strain (FMF361) have been described (Connolly et al., 2013). The same approach was used to disrupt *FUS1* (*PKS10*; FGSG_07798), *FUS8* (FGSG_07804) and *PKS5* (FGSG_17677) by insertion of the *neo* gene, which confers resistance to G418. Primers used for construction and validation of deletion strains are listed in Supplementary Table 1. Strains bearing deletions of transcription factor genes *ZC116* (FMF938) and *ZC117* (FMF939) were a kind gift from Yin-Won Lee and Hokyoung Son (Seoul National University, Korea) and were constructed as described (Son et al., 2011). Strains used for this study are listed in Supplementary Table 2; strains that are also part of a forward genetics mutant hunt for genes defective in silencing used to generate additional RNA-seq data will be described in detail in a separate manuscript (see also GEO accession number GSE131036).

Unless specified elsewhere, strains were grown in liquid YPD (0.3% yeast extract, 1% peptone, 2% dextrose) medium to collect vegetative tissue. To generate macroconidia, conidia or tissue from frozen stocks were inoculated into 50 ml flasks containing CMC (carboxymethylcellulose) medium (Cappellini and Peterson, 1965) and shaken at 150 rpm for 3–4 days at room temperature (RT, ~22 °C). Conidia were collected by filtration through cheesecloth and stored at -80 °C in 25% glycerol. Crosses were performed on carrot agar (Connolly et al., 2018) at RT, taking between 10 and 14 days. For metabolomics analysis, triplicate 50 ml cultures of PH1 and *kmt6* were grown for seven days in YPD broth in the dark. For SecMet isolation, cultures of YPD broth were inoculated with conidia and grown for seven days at 200 rpm at 21 °C.

2.2. RNA-seq analysis

Total RNA was isolated from 1 to 3 day old tissue by a previously described method (Connolly et al., 2013), and mRNA was isolated using a Poly(A) Purist MAG kit (Ambion). We removed DNA by treatment with RNase-free DNAase (Qiagen), followed by column clean-up according to manufacturer's instructions. cDNA was generated with Superscript III (Thermo) and either subjected to region-specific semi-quantitative PCR with gene-specific primers or used to make libraries for high-throughput sequencing. We used Illumina TruSeq RNA or SOLiD sample preparation kits to make RNA-seq libraries; cDNA was sequenced on Illumina HiSeq2000, Illumina HiSeq3000, or ABI SOLiD 5500xl genome analyzers. Data were analyzed as described previously (Connolly et al., 2013). In total, 68 new RNA-seq datasets (GEO accession number GSE131036) were compared to the previous datasets (SRA Bioproject PRJNA221153). In addition to mapping and RNA-seq analyses carried out as described (Connolly et al., 2013), we also manually curated biosynthetic gene clusters that were most recently described (Sieber et al., 2014), and added potential new gene clusters (Table 1).

2.3. General spectroscopic and chromatographic procedures

Circular dichroism and UV measurements were recorded using a JASCO J-815 spectropolarimeter. IR spectra were recorded on a Thermo Scientific Nicolet 6700 FT-IR spectrometer. NMR spectra were acquired on a Bruker Avance III 500 MHz or Bruker Avance III 700 MHz spectrometer, equipped with a 5 mm TXI probe or 5 mm BBO probe (500 MHz and 700 MHz) or TCI cryoprobe (700 MHz), with the residual solvent used as an internal standard (d6-DMSO 2.50/39.52 ppm; CDCl₃: 7.26/77.16 ppm; d4-methanol: 3.31/49.00 ppm, d5-pyridine: 8.74/ 150.35 ppm). Low-resolution ESI-MS and high-resolution TOF-MS (ESI) mass spectra were recorded on Agilent 1100 series LC with MSD 1946 and Agilent 1260 series LC with 6230 TOF MS, respectively. A Teledyne Isco CombiFlash Companion system was used for adaptive gradient. automated flash chromatography. Analytical HPLC was performed using an Agilent 1100 HPLC system equipped with a photodiode array detector. The mobile phase consisted of ultra-pure water (A) and acetonitrile (ACN) (B) with 0.05% formic acid in each solvent. A gradient method from 10% B to 100% B in 35 min at a flow rate of 0.8 ml/ min was used. The column (Phenomenex Kinetex C18, $5 \, \mu m \times$ 150 mm × 4.6 mm) was re-equilibrated before each injection, and the column compartment was maintained at 30 °C throughout each run. Semi-preparative HPLC (Phenomenex Kinetex C18, $5 \, \mu m \times$ $150\,\mathrm{mm} \times 10\,\mathrm{mm}$ column) utilized isocratic elution conditions or a gradient system with a flow rate of 4 ml/min on an Agilent 1100 HPLC system operating at room temperature equipped with a photodiode array detector. Preparative HPLC (Phenomenex Luna C18, $5\,\mu m$ \times 250 mm × 21 mm column) was conducted at room temperature, using isocratic elution conditions or a gradient system with a flow rate of 20 ml/min utilizing an Agilent 1260 Infinity series HPLC equipped with a diode array detector. Final compound isolations were performed utilizing HPLC-DAD. For each compound, the retention time from Fig. 1 was converted into the isocratic percentage for the organic solvent B or a shallow gradient starting from the eluting percentage B minus 10% to the eluting percentage B plus 10% over 20 min was used. All samples were filtered through a 0.45 µm nylon filter before LCMS and HPLC analysis. Analytical thin layer chromatography (TLC) was performed on pre-coated silica gel 60 F254 plates (Eppendorf). TLC plates were visualized by UV (254 and 360 nm), and by spraying with p-anisaldehyde solution followed by heating at 80 °C.

2.4. Metabolomics analysis

Triplicate cultures of WT and kmt6 grown in YPD medium were extracted with 50 ml ethyl acetate (EtOAc) at 200 rpm and ambient temperatures for 48 h. The organic phase was separated and washed

 Table 1

 H3K27me3 enrichment and expression as measured by RNA-seq of 76 known and predicted BGCs in F. graminearum.

BGC ^a	Signature ^b	Locus ID	Other names ^c	K27me3 present	Expression in WT	Increased expression in kmt6	Metabolite	References ^d
01	none ^e			+	no	no		
02	NPS8, NPS-like FAS	15673, 11656		+	no	yes	gramillin A, gramillin B	Bahadoor et al. (201
03	none			+	no	yes		
04	none			+	no	yes		
05	STC2	15742		_	no	no		
06	NPS16, NPS19,	15872, (11988 + 15676)		-	no	yes		
07	TPS, NPS-like	01738, 01743		+	yes	yes		
80	TPS, PKS11	01783, 01790	PKS25/FUM1	+	yes	yes		
)9	none			+	no	yes		
10	none			+	no	yes		
11	NPS-like	02251, 15967		+	no	yes		
12	none			+	no	yes		
13	PKS12	02324	PKS26/AUR1	+	yes	yes	aurofusarin	Malz et al. (2005)
14	none	FFUJ_12020		+	no	yes		
15	PKS4, PKS13, NPS15	17745, 15980, 02394	PKS22/ZEA2, PKS27/ZEA1	+	no	yes	zearalenone	Kim et al. (2005), Gaffoor and Trail (2006)
16	PKS15	04588	PKS29/PLSP1	+	no	yes		
17	NPS-like FAS	04333	-,	_	yes	yes		
18	PKS14	03964	PKS28/GRS1	+	no	yes	orcinol, orsellinic acid	Jorgensen et al. (201
19	none		., ., .	+	no	yes	, , , , , , , , , , , , , , , , , , , ,	0
20	none			+	no	yes		
21	NPS6	03747	SidD	_ f	yes	yes	triacetylfusarinine	Oide et al. (2006)
22	NPS-like	16213		+	no	yes	,	
23	TPS	03537	TRI5	+	no	yes	trichothecene	Proctor et al. (1995)
24	STC4	03494		+	no	yes	fusariumdiene, fusagramineol	Bian et al. (2018)
25	none			+	yes	yes		
26	PKS8	03340	PKS13/GPY1	+	no	yes	gibepyrones, prolipyrone	this study; (Westpha et al., 2018)
27	NPS-like	03257		+	no	yes		
28	DTC1	03066	CARB/al-2	+	yes	yes	carotenoids	Jin et al. (2010))
29	NPS-like	02873		+	yes	yes		
30	none			+	yes	yes		
31	PKS2	04694	PKS2, PKS30	+	no	yes		
32	none			+	no	yes		
33	NPS2	05372	SidC	_ g	yes	no	ferricrocin	Tobiasen et al. (200
34	PKS5	17677		+	no	yes		
35	NPS-like	16594		_	yes	no		
36	TPS	04694		+	no	yes		
37	NPS, NPS-like	06462, 12922		+	no	yes		
38	NPS10	06507		_	yes	no		
39	none			_	yes	no		
10	none	16070		+	yes	yes		
11 12	STC1 PKS10	16873 07798	FUS1	+	yes no	yes yes	fusarins (fusarin A, C, D), protofusarin ^h	Gaffoor et al. (2005
43	none			_	yes	no	F. 0103 mm 01	
14	PKS7	08795		_	yes	no		
45	none			_	no	no		
46	NPS-like FAS	17057		_	yes	no		
17	PKS6, NPS7	08208, 08209	NPS7, PKS23	+	no	yes	fusaristatin A	Sørensen et al. (201
18	STC5, NPS-like	08181, 08184	,	+	no	yes	tricinolonoic acid, tricinonoic acid, tricindiol, tricinolone	this study
19	none	08079	CYP53A6	+	no	yes	butenolide	Harris et al. (2007)
50	none			+	no	yes		
51	none			+	no	yes		
52	none			+	yes	yes		
53	PKS3	17168	PGL1	+	no	yes	perithecial pigment, bostrycoidins	Gaffoor et al. (2005 Frandsen et al. (201
54	none			+	yes	yes		
55	none			+	no	yes		
56	TPS	09381		-	yes	no		
7	none			-	yes	no		
58 59	TPS STC9	17725 10397	CLM1	_	no yes	no yes	culmorin	McCormick et al.
50	NPS-like, PKS9	10459, 10464	PKS24/FSL1	+	ves	ves	fusarielin	(2010) Sorensen et al. (201
50 51	PKS1, NPS18	17387, 13783	NPS18, PKS21	+	yes	yes no	14341101111	oorensen et al. (201
51 52	NPS-like	10617	19F510, FR521	+	yes yes	yes		
63	NPS1	11026		+	no no	yes	malonichrome	Oide et al. (2014)
				•		,		(continued on next p

Table 1 (continued)

BGC ^a	Signature ^b	Locus ID	Other names ^c	K27me3 present	Expression in WT	Increased expression in kmt6	Metabolite	References ^d
C64	NPS5, NPS9	17487, 10990		+	no	yes	fusaoctaxin	Jia et al. (2019)
C65	TPS	10933		_	yes	no		
C66	NPS14	11395		+	no	yes	chrysogine	Wollenberg et al. (2017)
C67	none			+	no	yes		
C68	PKS-like	07226	KSA1	_	yes	yes		
C69	STC6	11327		+	no	yes		
C70	NPS4	02315		+	yes	yes		
C71	NPS3	10523		_	yes	no		
C72	NPS11	03245		+	no	yes		
C73	NPS12	17574		+	no	yes		
C74	NPS13	13153		_	yes	yes		
C75	NPS17	10702		_	no	yes		
C76	PKS52 ⁱ	FG05_30424		ND	ND	ND		

^a Cluster designations C01 to C67 are as previously described (Sieber et al., 2014), C68 to C76 are designated here.

with a single 50 ml portion of deionized H₂O before drying in vacuo. Each extract was prepared to 10 mg/ml in 1:1 ACN:methanol (MeOH) for LCMS analysis. Each sample was analyzed in duplicate on an Agilent 1100 series LCMS platform. Positive mode ionization was found superior in detecting metabolites when compared to negative ionization mode and used for all further analyses; similar results have been previously observed by other groups analyzing microbial metabolites (Hou et al., 2012) (Nielsen et al., 2011). Data sets were exported from Agilent's Chemstation software as .netCDF files and imported into MZmine 2.21 (Pluskal et al., 2010). Peak picking was performed with established protocols (Abdelmohsen et al., 2014; Adpressa and Loesgen, 2016; Hou et al., 2012) resulting in 202 marker ions. Mass detection was centroid with 1E2 minimum height. Chromatogram building was limited to peaks greater than 0.1 min with $0.1 \, m/z$ tolerance and 5E2 minimum height. Data smoothing was performed at a filter width of 13. Chromatogram deconvolution utilized local minimum search with 50% threshold, 5 min search range, 25% relative height, 1E4 minimum abs. height, 2 minimum ratio of top/edge, and peak duration from 0.2 to 3 min. All treatments were then aligned and duplicate peaks combined with a tolerance of $0.1 \, m/z$ and $0.2 \, min$. Peak finder gap filling was performed with 75% shape tolerance and $0.1 \, m/z$ tolerance. Log-ratio analysis was carried out with MZmine's integrated statistical software (Pluskal et al., 2010). Ion abundance values were averaged over technical replicates, log-transformed to improve normality, and compared between the WT and *kmt6* cultures using a two-sample, two-tailed *t*-test. This analysis indicated that 44 chemical entities were more abundant while 22 were less abundant (p < 0.05) in the kmt6 mutant, and 104 were not significantly different.

2.5. Isolation and structure elucidation

For the preliminary metabolite isolation culture, 4 L of YPD broth was inoculated with *kmt6* conidia and grown in the light for 5 days at 200 rpm. The culture was extracted with 4 L EtOAc overnight. The organic layer was collected and dried *in vacuo* to yield 3.2 g. This

extract was separated by semiautomated flash column chromatography with an ISCO Combiflash on a 40 g silica column (Grace Reveleris) utilizing a gradient from 100% hexane to 100% EtOAc to 100% MeOH with adaptive gradient pausing. Seven fractions were combined by analysis of UV chromatograms at 254 and 280 nm and labeled as fractions 1–7. Final compound isolations were performed utilizing HPLC-DAD. Fusarins C, A, and D were isolated from fraction 2 and identified base on UV, LR-MS, and ¹H NMR compared to literature (Kleigrewe et al., 2012; Niehaus et al., 2013). Fusaristatin A was isolated from fraction 5 and its structure confirmed by HRMS and ¹H NMR (Shiono et al., 2007; Sørensen et al., 2014). Zearalenone was identified by LRMS, HRMS, UV, and retention time as compared with a standard (Cordier et al., 1990). Protofusarin and tricinolonoic acid were isolated from fraction 1.

A second 18 L culture of YPD broth with 50 g of XAD-7 resin (Acros) per liter was inoculated with conidia of kmt6 grown in the dark at 200 rpm for seven days. The XAD resin was removed by filtration and washed with 18 L of deionized H₂O. The resin was then stirred with 5 L acetone and MeOH. The organic extracts were combined and dried in vacuo to yield 44 g product. The culture extract was loaded onto 88 g silica (SiliaFlash P60, Silicycle) and subjected to vacuum liquid chromatography with step gradients of 99:1, 50:1, 30:1, 15:1, 9:1, 3:1, 2:1, 1:1, and 0:1 dichloromethane (DCM):MeOH and labeled as fractions 1–9. Fraction 6 (2.36 g) was further separated by semiautomated flash column chromatography with an ISCO Combiflash on a 12 g silica column (Grace Reveleris) utilizing a gradient from 100% hexane to 100% EtOAc to 100% MeOH with adaptive gradient pausing. Ten fractions were separated by analysis of UV chromatograms at 254 and 280 nm and labeled as fractions 6a-6j. Gibepyrone A was isolated from fraction 3. Related fusarpyrones A and B were isolated from fraction 6d. N-acetyltryptamine was isolated from fraction 6g. N-phenethylacetamide and N-ethylanthranilic acid were isolated from fraction 6c.

A separate 4 L culture of the *kmt6 fus1* double deletion mutant in YPD was grown to target compounds co-eluting with fusarin type compounds. The culture was grown and extracted as above to yield a

^b Signature genes belonging to the PKS, PKS-like, NRPS, NRPS-like, and STC groups are indicated and their current FGSG numbers shown as locus ID (omitting "FGSG_" for brevity). General references for signature gene assignments in *F. graminearum* follow previous systems (for TPS, (Wiemann et al., 2013); for NPS-like loci, (Sieber et al., 2014); for comprehensive PKS and NRPS numbering for the genus Fusarium, (Hansen et al., 2015).

^c Previous designation have been used for alternative PKS (Kroken et al., 2003; Wiemann et al., 2013) and gene names (Gaffoor et al., 2005), previous gene names have priority over "PKS" gene names.

d References relate to identification of metabolite or sorting of metabolite to BGC.

^e No homologs to known signature genes were found by BLAST searches.

f The NRPS gene is not covered by H3K27me3.

^g Only the promoter of the NRPS gene is enriched with H3K27me3.

h New compounds isolated and identified in this study are protofusarin, tricinolonoic acid, and tricinolone (shown in italics).

ⁱ BGC52 was identified in an Australian accession of *F. graminearum* (Gardiner et al., 2014) and is not found in the currently available genome sequence of the reference strain, PH-1.

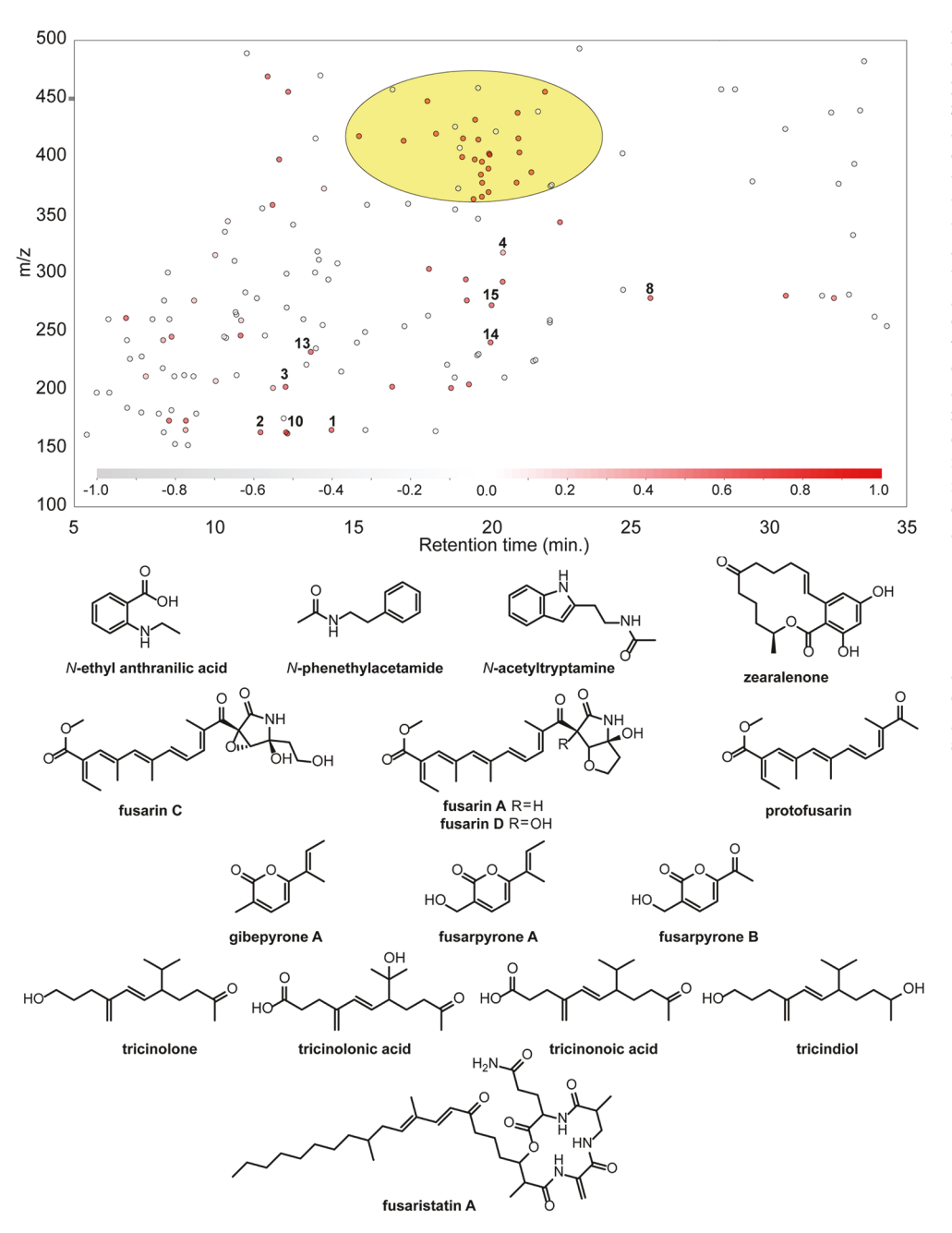


Fig. 1. Metabolomics-guided approach for analysis and isolation of compounds overproduced upon deletion of KMT6 in F. graminearum. Top panel: results from log-ratio analysis of LCMS data highlights SecMets overabundant in kmt6 (red dots) or wild type (gray dots). Overall, 170 chemical entities matched our statistically determined thresholds for inclusion in the log ratio analysis (see Methods and Materials). Of these, 44 entities were significantly upregulated in kmt6, 22 were significantly downregulated in kmt6 (p < 0.05), and 104 were not significantly changed according to our stringent criteria. Compounds isolated, and identified from the kmt6 mutant are numbered. The yellow shaded region indicates fusarin isoforms and MS fragment ions. Bottom panel shows compounds found in this study with numbers identifying location in log-ratio plot (top panel): N-ethyl anthranilic acid (1), N-phenethylacetamide (2), N-acetyltryptamine (3), zearalenone (4), fusarin compounds (5-7), protofusarin (8), gibepyrone A (9), fusarpyrones A and B (10, 11), tricinolone (12), tricinolonoic acid (13), tricinonoic acid (14), tricindiol (15), and fusaristatin A (16). (For interpretation of the references to colour in this figure legend, the reader is referred to the web version of this article.)

9.5 g extract and fractionated accordingly. Tricindiol was isolated from fraction 6d and tricinonoic acid and tricinolone from 6c by reverse phase semi-preparative HPLC. All computational methods, spectra, and other data supporting the identification of metabolites are supplied in the Supplemental Information.

3. Results and discussion

The single H3K27 methyltransferase in *F. graminearum*, Kmt6, is an important global repressor of secondary metabolism, and essential for normal development and cell differentiation (Connolly et al., 2013). In some species, like *F. fujikuroi*, Kmt6 is an essential protein and thus deletion mutants have not been generated (Studt et al., 2016). Reporting on changes in primary and secondary metabolism in *F. graminearum* after deletion of *KMT6* was the primary aim of this study. Twenty-two metabolites were identified. Ten of these are described from *F. graminearum* for the first time, and three are new metabolites which were characterized by extensive 1D and 2D NMR analysis paired

with high-resolution mass spectrometry. During our studies we refined the borders of currently annotated BGCs in *F. graminearum*; for example, some known BGCs are clearly split between H3K27me3-enriched and non-enriched loci, which are not co-regulated under the conditions used here, and which do not match other known clusters as predicted by the literature, or by analyses with antiSMASH (Weber et al., 2015; Blin et al., 2019) or SMURF software (Khaldi et al., 2010). Here, we report all results from studies that combine efficient chemical and genetic dereplication, i.e., by using gene deletion strategies that further enhance the utility of strains in which a global repressor has been removed. Thus, the various compounds described here fall into different groups, both in terms of strategy applied to identify and isolate new compounds, and in terms of novelty.

3.1. RNA expression data predict production of new metabolites

Previously we showed that deletion of *KMT6* resulted in upregulation of \sim 20% of all genes in the *F. graminearum* genome, many of which

are predicted to be involved in SecMet production (Connolly et al., 2013). To understand which metabolites may be overproduced, we extended and updated the annotation of BGCs that are affected by KMT6 deletion, supported by RNA-seq data from 68 additional mutant and WT strains (GEO accession GSE131036), following the nomenclature suggested by others (Brown and Proctor, 2016; Hansen et al., 2015; Sieber et al., 2014; Wiemann et al., 2013). Of the now 76 predicted clusters, 52 contain "classic" signature genes for non-ribosomal peptide synthetases (NRPS or NPS), terpenoid synthases (TPS), or polyketide synthases (PKS). The remaining clusters were defined by coexpression under various environmental conditions and contain genes for tailoring enzymes or cytochrome P450 nomenclature suggested by others (Brown and Proctor, 2016; Hansen et al., 2015; Sieber et al., 2014; Wiemann et al., 2013). These clusters may also contain genes for "ribosomally synthesized and post-translationally modified peptides" (RiPPs; (Vogt and Künzler, 2019), about which not much is known in Fusarium. Of 21 BGCs free of H3K27me3, five were not expressed in WT under any of our growth conditions (low or high nitrogen and low or high carbon) but two of these BGCs were de-repressed in the kmt6 mutant, suggesting an indirect effect of kmt6 deletion. Of 55 BGCs with H3K27me3 enrichment, 40 are transcriptionally silent in WT but 38 are expressed in kmt6. In summary, of the 76 BGCs annotated here, 59 (78%) are newly expressed or have higher transcript levels in kmt6 compared to WT (Table 1).

Based on the enrichment with H3K27me3 and co-expression data we annotated additional BGCs (C68-76; Table 1). Among the 12 BGCs encoding "NPS-like" proteins, there are five Fub8- or MxcG (myxochelin iron transport)-related synthetase (C22, C27, C48, C60, C62), three fatty acid synthase (FAS)-like NPS (C2, C17, C46), and three acetyl-CoA synthase- (C7, C37) or phenylacetyl-CoA ligase-related proteins (C29). The newly delineated BGCs include a previously described PKS-like gene, KSA1 (Gaffoor et al., 2005), the BGC with the sesquiterpene cyclase STC6 (C69), known to generate caryophyllene (Wiemann et al., 2013), and BGCs that encode NPS4, NPS3, NPS11, NPS12, NPS13, and NPS17 (C70-C75; Table 1).

3.2. Metabolomics-based chemical screening

To harness the power of our genetic de-repression system, and to identify elusive natural products, we turned to metabolomics-based analysis of LCMS data to identify the most abundant metabolites, which we developed as a simple yet powerful tool for the analysis of chemical profiles of fungi that were challenged by environmental (Adpressa and Loesgen, 2016) or chemical stressors (Adpressa et al., 2017). Here, LCMS-based log-ratio analysis was employed to identify metabolites which were overproduced in *kmt6* compared to WT. Organic extracts of *kmt6* and WT were prepared in biological triplicate and subjected to LCMS analysis in technical duplicate. LCMS profiles for each replicate were imported into MZmine 2 for peak binning, followed by log-ratio analysis with the MZmine 2 integrated statistical software package (Pluskal et al., 2010), and the relative expression plot was used to identify metabolites that exhibited high abundance in *kmt6* but not in WT (Fig. 1; a base peak chromatogram is shown in Fig. S71).

3.3. Overexpression of primary metabolites in kmt6

In some cases, the absence of Kmt6 alone resulted in sufficient overexpression of metabolic pathways that allowed identification of metabolites previously unknown from *F. graminearum*. We identified *N*-ethyl anthranilic acid by 2D NMR, isolated from *kmt6* extracts (Fig. 1, Figs. S1-5). Though anthranilates are common both as primary metabolites and building blocks in more complex natural products in fungi, to the best of our knowledge, this is the first time *N*-ethyl anthranilic acid has been isolated as a natural product. WT did not produce *N*-ethyl anthranilic acid, which was confirmed by UV/retention time analysis and Extracted Ion Chromatography (EIC) at 166.2 *m/z*. Because the *N*-

ethyl is a surprising functionality, more common in industrial products than natural occurring metabolites, media blanks as controls as well as culture extracts of three additional fungi (Aspergillus terreus, Chalara sp., Phoma sp.) grown on YPD were analyzed by EIC for the presence of Nethyl anthranilic acid. Only F. graminearum kmt6 extract contained this compound, suggesting that it is biologically synthesized. Recent studies with several fungi showed that anthranilic and pyruvic acid are used for the biosynthesis of chrysogine, which is catalyzed by NRPS14 in F. graminearum (Wollenberg et al., 2017). Our observation of an increase in N-ethyl anthranilic acid in kmt6 suggests that even though NPS14 is overexpressed in the mutant, potentially too much precursor is present to be synthesized into chrysogine. Even though we looked for chrysogine (m/z 191.08 for $M+H^+$), the corresponding ions were below the statistically significant threshold for our log ratio analyses, even though they were increased when compared to WT.

Both *N*-phenethylacetamide and *N*-acetyltryptamine are detectable by UV, retention time, and EIC in WT cultures, but are overexpressed twenty- and two-fold, respectively, in *kmt6* cultures. *N*-phenethylacetamide was isolated and identified by extensive 2D NMR spectroscopy (Fig. 1, Figs. S6-9). It has not been reported as a metabolite from *Fusarium*, but is known from *Protostropharia semiglobata* (Reinoso et al., 2013), *Tricladium* sp. (Zou et al., 2011), and a marine fungus (Wu et al., 2009). *N*-acetyltryptamine was identified by matching spectroscopic data (Figs. S10–12) of *N*-acetyltryptamine isolated from *F. incarnatum* (Li et al., 2008).

3.4. Overexpression of BGCs with known products: fusarins, zearalenones, and fusaristatin \boldsymbol{A}

Based on our RNA-seq analyses we expected several known products of BGCs to be significantly overproduced. The fusarin gene cluster (C42) lies on chromosome 4, which contains 17 of the 76 BGCs in F. graminearum (Fig. 2A). In contrast to its distribution in plants, animals or Neurospora (Jamieson et al., 2013), H3K27me3 is most often present in large blocks in F. graminearum (Connolly et al., 2013), and the middle 400 kb of chromosome 4 (8.1 Mb) shows dense enrichment with H3K27me3 but a dearth of H3K4me2, a histone modification correlated with gene expression (Fig. 2B). RNA-seq showed that few genes in this region are expressed in WT, while many, including the three BGCs covered by H3K27me3 (C40; C41, including STC1; C42 including PKS10FUS1), are specifically upregulated in kmt6 (Fig. 2B). Within the predicted fusarin gene cluster, eight of the eleven proposed cluster genes show increased mRNA levels compared to WT (Fig. 2C), confirming our previous RNA-seq analyses that showed upregulation by ~60-fold (Connolly et al., 2013). The first three genes (FGSG_07795, FGSG_16897, FGSG_07797) of the cluster as defined previously (Sieber et al., 2014), however, show no difference in gene expression and should therefore no longer be considered as part of a co-regulated cluster C42; all encode conserved predicted proteins with no demonstrated function.

When compared to WT, dozens of m/z entities were identified as unique or increased in area by either HPLC-DAD, LCMS, or log-ratio analyses from kmt6 cultures grown in YPD liquid medium (Fig. 1, highlighted region). HPLC-DAD analysis indicated that the majority of these metabolites belonged to the same structural class. Analyses of the major peak revealed fusarin C as the primarily overexpressed metabolite (confirmed by HRMS ¹H NMR and HRMS (432.2001 [M + H] ⁺ C₂₃H₃₀NO₇, calc'd for 432.2020) and NMR; Figs. S13-15). Two additional fusarins were identified (fusarin A and fusarin D, see LRMS and NMR analysis; Figs. S16-20). Overall, fusarins are ~600-fold more abundant in kmt6 cultures based on ion count determined here. For each of the three fusarins many E/Z isomers have been reported, and isomerization in the presence of UV light has been widely observed (Kleigrewe et al., 2012). Based on the similar m/z values and UV spectra, as well as the structural conformation of fusarins A, C, and D isolated here, the entities within this cluster were all assigned as fusarin analogs and fragment ions (Fig. 1, highlighted region).

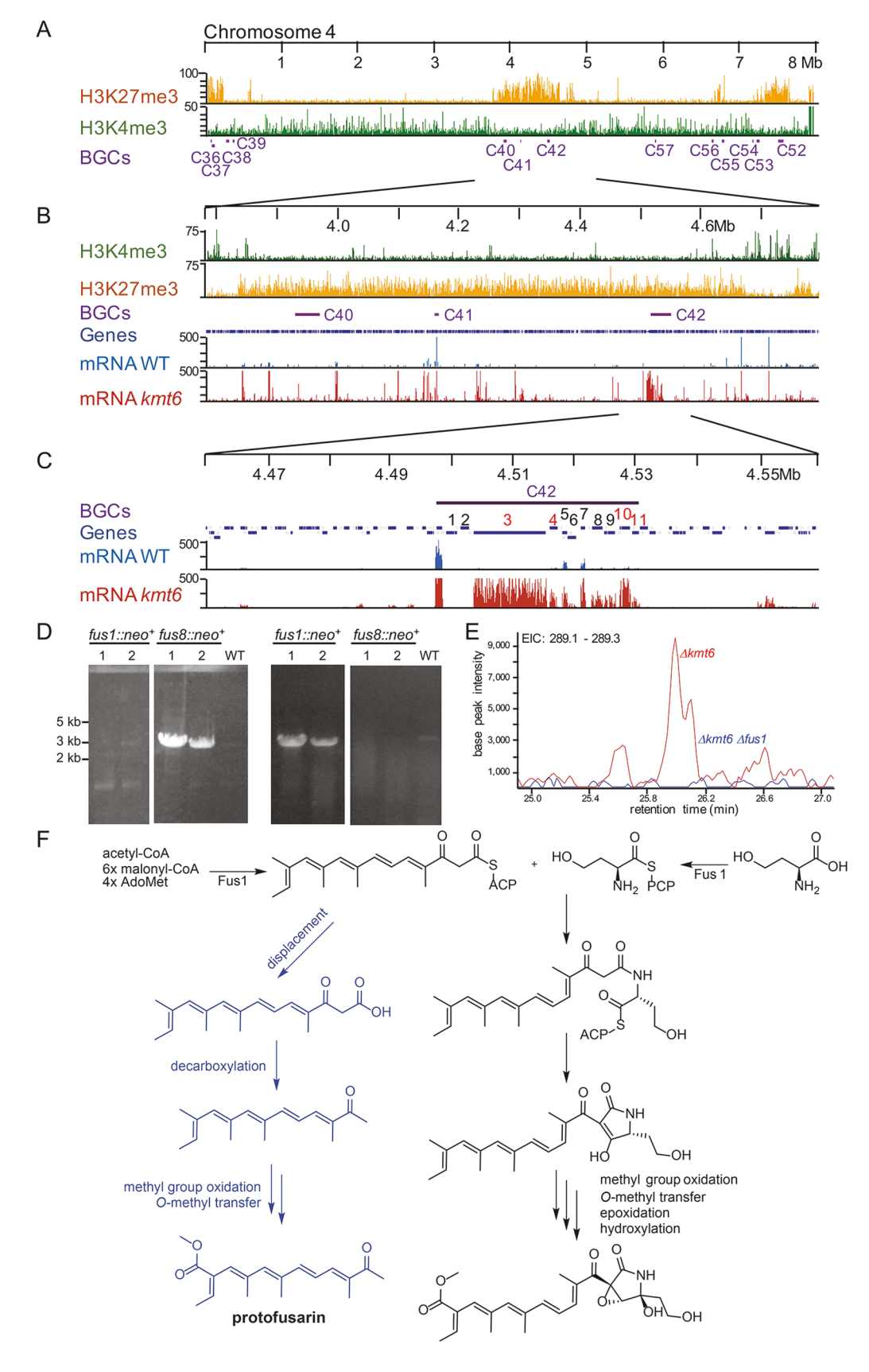


Fig. 2. Chromatin marks on F. graminearum chromosome 4, location of biosynthetic gene clusters (BGCs), expression in wild-type and kmt6 strains, structure of the fusarin BGC (C42), and proposed biogenesis of protofusarin. (A) Chromatin marks and BGCs on chromosome 4. Most BGCs are located in regions with H3K27me3 (orange) enrichment. Gene-rich regions are enriched with H3K4me2 (green). (B) Silent regions occur in large blocks, often extending hundreds of kilobases (kb). This view shows that many, but not all genes (dark blue) enriched with H3K27me3 are upregulated after deletion of KMT6. mRNA levels in WT (blue) and Δkmt6 (maroon) were determined by strand-specific RNA-seq. (C) Expression landscape around the fusarin BGC (C42; genes are numbered: 1, FGSG_16897; 2, FGSG_07797; 3, FUS1/PKS10; FGSG 07798. FGSG_13222, FUS2; 5, FGSG_13223, FUS3; 6, FGSG_07800, FUS4; 7, FGSG_07801, FUS5; 8, FGSG_07802, FUS6; 9, FGSG_07803, FUS7; 10, FGSG 07804, FUS8 cytochrome P450; 11, FGSG_07805; gene numbers in red indicate requirement for fusarin production in F. fujikuroi (Niehaus et al., 2013). The first, unlabeled gene (FGSG_07795) in C42 (defined in (Sieber et al., 2014) is not differentially expressed and thus should not be part of this BGC; it encodes a conserved predicted protein. Genes 5 (FUS3) and 7 (FUS5) show only minor increase in expression in $\Delta kmt6$; neither gene is required for fusarin synthesis in F. fujikuroi. Genes 1 and 2 are not induced in kmt6 or under growth conditions with varied nitrogen and carbon sources; they encode conserved predicted proteins of unknown function. Similarly, functions for genes 6, 8, and 9 remain to be discovered. (D) Two genes, FUS1/ PKS10 and FUS8, were disrupted by integration of a neo gene into a Δkmt6::loxP strain (Connolly et al., 2018), resulting in G418-resistant transformants that lacked fusarin production in Δkmt6. (E) Protofusarin production is high in \(\Delta kmt6 \) strains (red line; peak at 26.0 min) but abolished in strains in which both kmt6 and fus1 have been deleted (blue line; Δkmt6 $\Delta fus1$). (F) Biogenesis of fusarins (black), as well as the proposed biosynthesis of the newly identified protofusarin (blue) via polyketide only intermediates. (For interpretation of the references to colour in this figure legend, the reader is referred to the web version of this article.)

In addition to the expected and well known fusarins, a new metabolite was identified. This metabolite was selected as target for isolation based on the given m/z value of 289.2 at 26 min in the LCMS analysis (Fig. 1; a base peak chromatogram is shown in Fig. S71). Fraction one contained a compound with matching retention time and m/z with an

HRMS formula of $C_{18}H_{24}O_3$ (289.1784 m/z [M+H]⁺ calculated for 289.180). The simple UV spectrum ($\lambda_{max} = 347$ nm) bore a striking similarity to the fusarin class of compounds, yet no fusarin published matched the molecular formula obtained by HRMS. The 1H NMR spectrum contained a series of downfield resonances almost identical to

fusarin C, yet lacked the resonances associated with the homoserine moiety usually present in fusarins. A methylketone resonance at 199.9 ppm in the HMBC spectrum indicated truncation of the polyene moiety at the location of the NRPS-PKS connection point. Full 2D NMR assignment (Figs. S21-25) of the structure revealed a new metabolite of the fusarin pathway, which we named "protofusarin".

We propose that protofusarin is derived by a hypothetical pathway involving the PKS, Fus1; the usual biosynthetic pathway is well-studied in F. fujikuroi (Niehaus et al., 2013). In support of this hypothesis, protofusarin production was dependent on the presence of the fus1 gene (Fig. 2E). Spontaneous decarboxylation of the PKS product would lead to a polyene that is further processed by the cytochrome P450 and Omethylation enzymes (encoded by fus8 and fus9, respectively) to yield protofusarin. The tailoring enzymes may be promiscuous and process protofusarin in the same manner as standard fusarin analogs. Notably, the homoserine moiety does not seem to be required for oxidative processing. Although previous shunt metabolites of this pathway have been reported, protofusarin is here newly described. This finding exemplifies one general consequence of genetic or chemical perturbation, namely that by overexpression of BGCs the normal substrate-product regulation may suffer. The availability of precursors and co-factors strongly affects relative abundance of intermediates or final products, and imbalance of supply may give rise to the formation of new scaffolds and unexpected "natural" products (Adpressa et al., 2017).

We also wished to assess how well transcription level correlated with metabolite abundance. In contrast to the highly over-expressed fusarin BGC (C42), the zearalenone BGC (C15) showed little overexpression by RNA-seq in *kmt6* YPD cultures. The log-ratio plot indicated the presence of the parent zearalenone ion (Fig. 1) in fourfold greater abundance than in WT, which was confirmed by isolation and comparison with a zearalenone standard. Cultures of *kmt6* grown on barley-spelt medium produced even more zearalenone congeners. In total six known zearalenone isoforms were identified by various spectroscopic techniques including NMR, MS, and UV (Figs. S26-40). This analysis showed that the coupled RNA-seq and log-ratio analyses were sensitive enough to detect even small increases in metabolite abundance.

During the metabolomics-guided isolation of new metabolites from kmt6, we also discovered and isolated a compound with a formula of $C_{36}H_{58}N_4O_7$ (659.4355 m/z [M+H] + calculated for 659.4380) as determined by HRMS. Extracted ion chromatograms indicated that the compound was only produced in kmt6 cultures but that it ionized poorly in positive electron-spray ionization mode and therefore was barely detectable in the log-ratio analysis (Fig. 1). Only $100\,\mu g$ of the metabolite was isolated, limiting NMR analysis to HRMS and ¹H analysis (Fig. S41). A review of the literature suggested fusaristatin A, a cyclic lipopeptide as the likely compound (Shiono et al., 2007; Sørensen et al., 2014), which was confirmed by HRMS and ¹H NMR. Our RNA-seq data showed that none of the genes required for the fusaristatin A BGC (C47) are expressed in WT, while all C47 genes are overexpressed in kmt6 (Fig. 3A). Previously, extensive testing of different growth media and culture conditions were necessary to yield sufficient fusaristatin A (Hegge et al., 2015; Sørensen et al., 2014). Here, we found production of fusaristatin A in kmt6 in all growth conditions, and we confirmed that pks6 was required for fusaristatin A biosynthesis in the kmt6 genetic background by generating a pks6 kmt6 double mutant (Fig. 3B).

3.5. Identification of fusarpyrones A and B, produced by PKS8

Further analysis of the log-ratio plot for newly and overproduced compounds from kmt6 focused on a compound eluting at 12 min with an m/z value of 181.1. Subsequent isolation of the compound from fraction 6d resulted in assignment of the structure as fusarpyrone A. Fusarpyrone B and the parent metabolite, gibepyrone A (aka "fusalanipyrone"; (Abraham and Arfmann, 1988; Abraham et al., 1990; Janevska et al., 2016) were isolated and fully elucidated by 2D NMR (Figs. S42-50). Fusarpyrone B is poorly detected in positive ionization mode and

therefore did not readily appear in the log-ratio analysis. In WT, low levels of gibepyrone A were detectable but we never found fusarpyrone A and B in these extracts.

All three compounds have been previously reported from *F. solani* (Trisuwan et al., 2013), and gibepyrone A was identified from *F. fujikuroi* (Janevska et al., 2016) and recently (concurrent with our studies) from *F. graminearum* (Westphal et al., 2018). Several *F. graminearum* PKS contain the *S*-adenosylmethionine (SAM)-dependent methyltransferase domain necessary for the biosynthesis of methylated pyrones (Abraham et al., 1990; Hansen et al., 2015). *PKS8* (FGSG_03340) encodes a well-conserved reducing iterative type I PKS containing a keto-synthase (KS), an acetyltransferase AT), a dehydratase (DH), a methyltransferase (cMT), an enoylreductase (ER), a ketoreductase (KR) and an acyl carrier protein (ACP). *PKS2* (FGSG_04694) has the same domain structure, as does *PKS5* (FGSG_17677), which encodes a less conserved PKS with the same domains but also including a C-terminal carnitine acyltransferase domain of unknown function (Brown et al., 2012; Hansen et al., 2015).

Our RNA-seq data for *PKS8* match the production profile observed for gibepyrone A, with no or low expression in WT, but enhanced expression in *kmt6* (Fig. 4A). Our data confirm results obtained when *PKS8* was expressed from a constitutive promoter, which resulted in expression of gibepyrones (Westphal et al., 2018). In that study, gibepyrones D and G were the most abundant metabolites detected, presumably products of non-specific cytochrome P450 action to detoxify gibepyrone A. In *F. fujikuroi*, *PKS8* (*GPY1*; FFUJ_12020) forms a two-gene cluster with an ABC transporter gene (*GPY2*; FFUJ_12021) that is co-regulated with *PKS8/GPY1* and also directly or indirectly affects PKS regulation. This transporter gene is missing from *F. graminearum* and related species, suggesting the need for gibepyrone A detoxification (our analyses and Westphal et al., 2018).

In addition to gibepyrone A, we identified two additional pyrones, fusarpyrone A and B. Gibepyrone F, bearing a similar ketone functionality as fusarpyrone B, may be derived non-enzymatically from gibepyrone A (Janevska et al., 2016) but fusarpyrone A was not reported from *F. fujikuroi*, and it differs from gibepyrone A by a hydroxyl group. This oxidized methylene moiety is likely to arise from cytochrome P450 monooxygenase activity which may be cluster-independent, as was the case for the oxidized prenyl moieties in gibepyrones B-D in *F. fujikuroi* (Janevska et al., 2016). Disruption of the *PKS8* gene resulted in absence of gibepyrones A (Fig. 4C). Based on all our data it seems likely that both fusarpyrones are derived from Pks8 followed by oxidative tailoring.

Surprisingly, deletion of *PKS5* in the *kmt6* genetic background appeared to reduce the levels of fusarpyrones and gibepyrone A, even though *PKS5* was not highly expressed in *kmt6* (data not shown). Little is known about this PKS. While conserved genes had been reported from *F. graminearum* and several other species, it was suggested to be absent from *F. verticillioides*, *F. solani*, *F. oxysporum* and *F. fujikuroi* (Hansen et al., 2015). Based on our recent searches, homologs are present in many strains of *F. oxysporum* as well as *F. fujikuroi* (e.g., KSU X-10626, locus ID LW93_15044) (Chiara et al., 2015).

In summary, by overexpression and isolation from *kmt6* extracts, three pyrone derivatives of gibepyrone A and fusarpyrone A and B have been identified in *F. graminearum*, and their structures fully elucidated by 2D NMR. Based on expression and genetic data, Pks8/Gpy1 is the enzyme responsible for the production of all three pyrones, supported by recent studies in *F. fujikuroi* (Janevska et al., 2016) and *F. graminearum* (Westphal et al., 2018).

3.6. Elimination of fusarin production by genetic dereplication

We showed that fusarins are the predominant class of compounds overexpressed in *kmt6*. To eliminate fusarin production and thus enable the screening for newly expressed metabolites in *kmt6*, a strategy called "genetic dereplication" (Chiang et al., 2009), we attempted to cross *kmt6* to strains carrying a disrupted fusarin BGC signature gene, *FUS1/PKS10*, encoding the PKS, Fus1 (Gaffoor et al., 2005). *Fusarium graminearum* is a

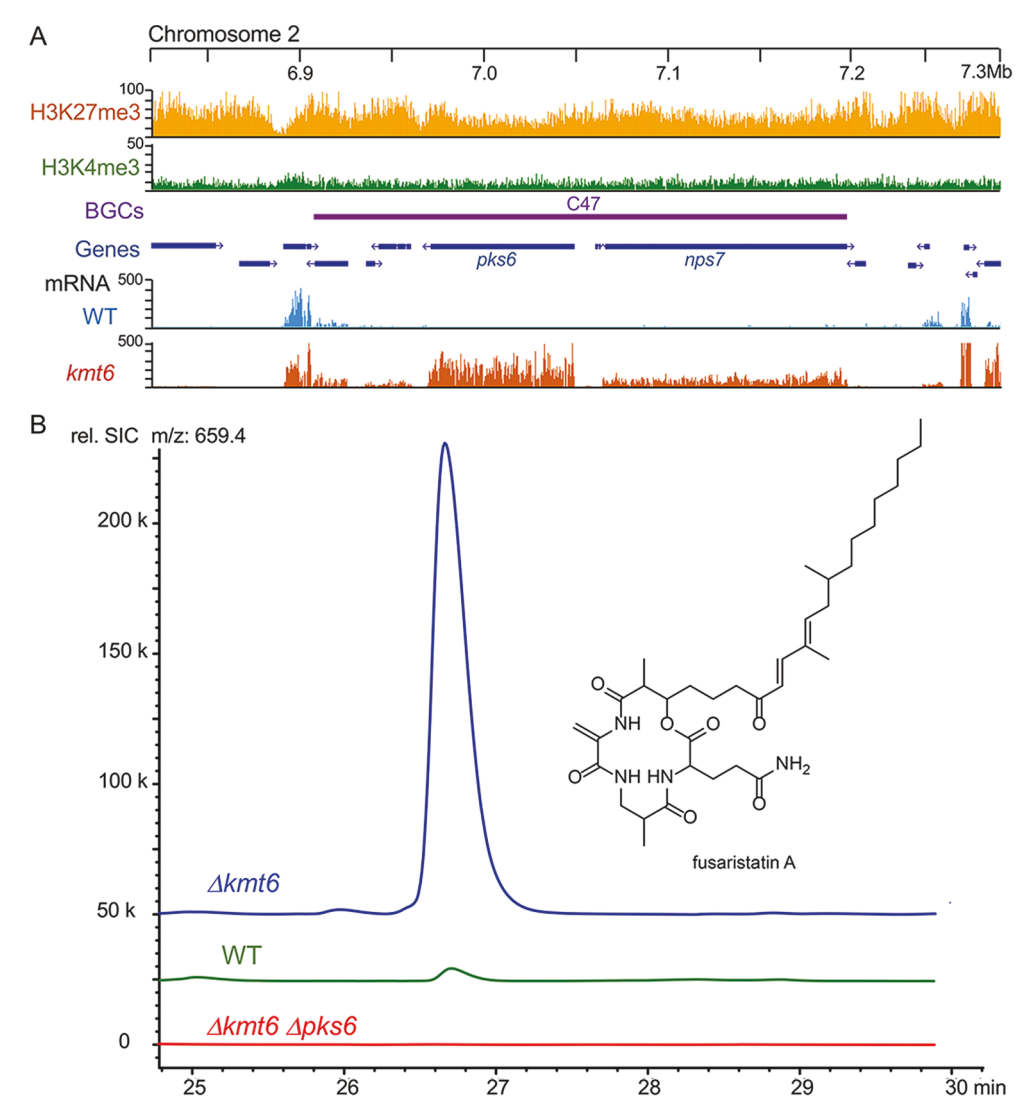


Fig. 3. Pks6 (C47) is required to synthesize fusaristatin A. (A) Chromatin environment, BGCs, genes, and RNA-seq of WT and Δkmt6 for C47 (see legend for Fig. 1). (B) LCMS analysis of the single Δkmt6 and the double Δkmt6 mutant at SIM m/z 659.4 in positive mode indicated complete removal of fusaristatin A production in the double deletion mutant, while fusaristatin A production is greatly increased in the Δkmt6 mutant when compared to WT.

homothallic, or self-fertile, species and thus does not require a partner of opposite mating type, as heterothallic fungi do. After outcrosses, recombinants, in this case kmt6::neo fus1::hph strains, can be isloated when selecting on medium containing both hygromycin and G418. Here, we found that kmt6 is female sterile (i.e., crosses can only be carried out with kmt6 spores as "male" or nucleus donor strain). The fus1 cultures did not show overt phenotypes on YPD or minimal medium but to our surprise we found that *fus1::hph*⁺ strains were sterile, both when used as recipient ("female") or donor ("male") strain. We next generated gene deletions in the kmt6 background, deleting independently both FUS1 and the nearby FUS8 gene, encoding a cytochrome P450 (Fig. 2D), to test whether the sterility effect was limited to FUS1 deletion. In F. fujikuroi, both genes are required for fusarin C production, where Fus1 generates prefusarin and Fus8 carries out successive oxidation reactions at C-20 (Niehaus et al., 2013). We found that both FUS1 and FUS8 are required for fertility in F. graminearum, which suggests a previously unsuspected function for fusarins in sexual development.

3.7. Discovery of two new sesquiterpenes, tricinolone and tricinolonoic acid

We used double deletion mutants (kmt6 fus1) to detect and isolate sufficient quantities of new compounds that co-eluted and were masked by the high abundance of fusarin isoforms in WT and in kmt6 single mutants. Log-ratio analysis provided several additional target compounds co-eluting with fusarin-type metabolites. Based on their m/z values, these metabolites did not appear to be fragments or previously unidentified shunt metabolites associated with fusarin. We grew the kmt6 fus1 mutant in four liters of YPD for a more expedient isolation of these metabolites. Extensive normal and reverse phase chromatography efforts yielded two compounds with a single UV maximum at 238 nm and m/z values of 241.2 and 275.2, matching the log-ratio peaks identified around 20 min. Characterization by 2D NMR revealed tricinonoic acid and tricindiol (Table 2, Fig. S51-58), previously reported from F. trinctium (Bashyal and Leslie Gunatilaka, 2010).

Based on this information, we scanned the list of BGCs in *F. graminearum* to assign the most likely gene cluster responsible for production of these sesquiterpenes. BGC C48 had been predicted to contain 19 genes, including the TPS *STC5* and an NRPS-like protein (Sieber et al., 2014) (Table 1), and it contained several genes predicted to encode cytochrome P450 enzymes that would be required for the production of the observed linear sesquiterpenes. Our RNA-seq data revealed that not all 19 genes are co-regulated under our conditions (Fig. 5A). The genes for the putative sesquiterpene cyclase (*STC5*, FGSG_08181), and the NRPS-like protein (FGSG_08184) are near those of two putative transcription factors (*ZC116* and *ZC117*). To determine whether the two transcription factors controlled biosynthesis of the

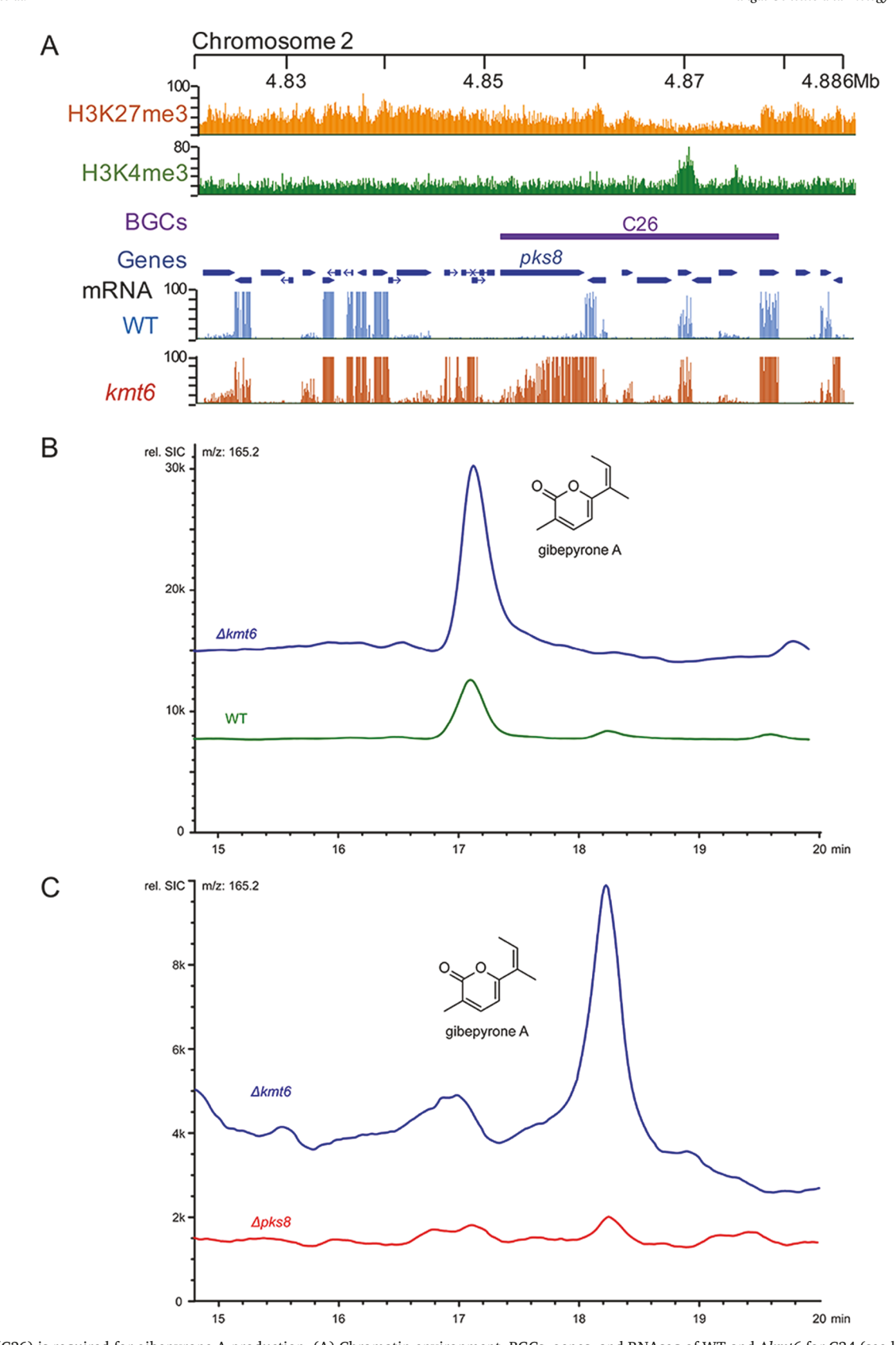


Fig. 4. Pks8 (C26) is required for gibepyrone A production. (A) Chromatin environment, BGCs, genes, and RNAseq of WT and $\Delta kmt6$ for C34 (see legend for Fig. 1), showing that *PKS8* is upregulated in the $\Delta kmt6$ mutant. (B) LCMS analysis of extracts from $\Delta kmt6$ and WT at SIM m/z 165.2 in positive mode indicated increased gibepyrone A production. (C) LCMS analysis of extracts from $\Delta kmt6$ and WT at SIM m/z 165.2 in positive mode showed that disruption of *PKS8* abolished production of gibepyrone A.

Table 2
Structures and NMR data for tricinolone, tricinolonoic acid, tricinolonic acid, and tricindiol.

	$\begin{array}{c ccccccccccccccccccccccccccccccccccc$		HO OH OH		0 H0 0 14 ^a		но ОН 15 ^b	
Position	$\delta_{\rm H}$	$\delta_{\rm c}$	δ_{H}	$\delta_c^{\ \sharp}$	δ_{H}	$\delta_{\rm c}$	$\delta_{\rm H}$	$\delta_c^{ \ddagger}$
1	3.69 t (6.4)	62.8, CH ₂		175.5, C _q		179.0, C _q	3.69 t (6.5)	62.8, CH ₂
2	1.76 m	31.4, CH ₂	2.56 br s	32.4, CH ₂	2.54 br s	33.0, CH ₂	1.72 m	32.3, CH ₂
3	2.28 t (7.8)	28.6, CH ₂	2.56 br s	26.6, CH ₂	2.54 br s	27.1, CH ₂	2.29 t (7.7)	28.6, CH ₂
4		145.7, C _q		143.6, C _q		144.1, C _q		147.0, C _q
5	5.98 d (15.8)	133.6, CH	6.1 d (15.8)	135.3, CH	5.99 d (15.8)	133.2, CH	6.01 d (15.8)	134.2, CH
6	5.42 dd (15.8, 9.4)	132.0, CH	5.5 dd (15.8, 9.4)	129.6, CH	5.41 dd (15.8, 9.4)	132.1, CH	5.52 dd (15.8, 9.4)	133.6, CH
7	1.76 m	49.8, CH	1.96 m	54.9, CH	1.77 m	49.7, CH	1.79 m	51.4, CH
8	1.76 m, 1.51 m	26.4, CH ₂	1.99 m, 1.48 m	23.1, CH ₂	1.77 m, 1.50 m	26.4, CH ₂	1.62 m, 1.26 m	29.4, CH ₂
9	2.36 m	42.2, CH ₂	2.41 m, 2.37 m	42.0, CH ₂	2.36 m	42.2, CH ₂	1.37 m	38.6, CH ₂
10		209.5, C _q		209.9, C _q		209.6, C _q	3.68 sext. (6.2)	68.7, CH
11	2.10 s	30.3, CH ₃	2.11 s	29.9, CH ₃	2.11 s	30.3, CH ₃	1.31 d (6.2)	23.3, CH ₃
12	4.93 br s, 4.91 br s	114.0, CH ₂	5.02 s, 4.98 s	115.0, CH ₂	4.96 s, 4.91	114.4, CH ₂	4.91 [‡] , 4.89 [‡]	$114.0, CH_2$
13	1.61 oct. (6.7)	32.5, CH		72.3, C _q	1.61 oct. (6.7)	32.5, CH	1.63 oct. (6.7)	33.3, CH
14	0.89 d (6.7)	20.9, CH ₃	1.21 s	26.6, CH ₃	0.89 d (6.7)	20.9, CH ₃	0.91 d (6.7)	21.2, CH ₃
15	0.84 d (6.7)	19.4, CH ₃	1.18 s	27.3, CH ₃	0.84 d (6.7)	19.4, CH ₃	0.86 d (6.7)	19.4, CH ₃

NMR spectra of compounds were recorded in CDCl₃ at 500 MHz for proton^a, 800 MHz for tricinolonoic acid^b, and 700 MHz in d₄-methanol for tricindiol^c.

sesquiterpene compounds identified here, we used strains from a transcription factor gene deletion library in which either ZC117 or ZC116 had been deleted (Son et al., 2011), and compared production of sesquiterpenes by these strains to expression in WT and kmt6. LCMS analyses of WT, kmt6, zc117, and zc116 strains showed that WT produced low levels of tricinonoic acid, which were increased in kmt6 and abolished in both transcription factor deletion strains (Fig. 5B).

During the isolation of tricindiol and tricinonoic acid, another metabolite with 13.5 min retention time in the log-ratio plot and with an m/z value of 251.2 ([M-H₂O+H]⁺) drew our interest. It seemed to be related to tricinonoic acid with a UV profile maximum at 232 nm. HRMS analysis revealed the molecular ion for the compound to be 291.1553, corresponding with a molecular formula of C₁₅H₂₄O₄Na⁺ (calculated for 291.1570). Comparison of the ¹H NMR spectrum with that of tricinonoic acid displayed a downfield shift for the methyl signals corresponding to the isopropyl side chain, as well as a loss of coupling between H-11/12 and H-10. Analysis of the HMBC spectra indicated C-13 was shifted in the new compound to 72.6 ppm, indicating the position was possibly hydroxylated. With the remaining signals almost unchanged, the structure was assigned as a new sesquiterpene, named tricinolonoic acid (Table 2, Figs. S59-61). Further chemical screening disclosed the presence of an additional congener with an m/z value of 239.2 and a simple UV spectrum with a maximum at 238 nm. ¹H and ¹³C spectra exhibit nearly identical signals as found for tricinonoic acid and tricindiol (Table 2, Figs. S62-66). Here, features of tricinonoic acid, a ketone ¹³C NMR shift at 209.4 ppm, and tricindiol, a hydroxyl bearing carbon at 62.7 ppm, are combined in tricinolone, a new, possible biosynthetic intermediate of tricindiol and tricinolonoic acid.

The absolute configuration of tricindiol was previously assigned by a combination of Mosher-ester NMR analysis for the C-10 hydroxyl functionality, and *J*-based analysis for the isopropyl moiety at position C-7 (Bashyal and Leslie Gunatilaka, 2010). We decided to utilize ECD analysis combined with computational prediction of the chiroptical properties of the new tricinolone and the co-isolated tricindiol and tricinonoic acid to verify their absolute configuration. Insufficient material was available for ECD experiments and therefore the absolute configuration could not be assigned. We turned to DFT-based computational ECD spectra, which indicated that tricinolone and tricinonoic acid exhibit the *S* configuration at the C-7 position (Figs. S67-68) in agreement with previously results (Bashyal and Leslie Gunatilaka, 2010); however, the ECD spectrum for tricindiol suggests that the

configuration at C-7 may be changed to 7-R (Figs. S69, S70). The switch in stereo configuration at C-7 represents an unusual find as most fungal sesquiterpene cyclases reported to date appear to exhibit stereospecificity in their product (Lopez-Gallego et al., 2010; Schmidt-Dannert, 2015). Further studies are necessary to assign the absolute configuration of these compounds with confidence.

In *F. fujikuroi* two TPS-containing BGCs with similar proposed activities as *F. graminearum* Stc5 have recently been studied. The BGC with the closest *STC5* homolog is syntenic with four genes in C48 (Fig. 5C), but four flanking genes are shuffled and inverted (Fig. 5 C). The gene from the reference strain (IMI58289), contains a mutation in the highly conserved NSE triad, where an asparagine is mutated to a lysine (N288K), rendering *F. fujikuroi STC5* inactive. Replacement with the *STC* gene from *F. mangiferae*, which lacks the N288K mutation, resulted in mRNA expression but the major metabolite, (1R,4R,5S)-guaia-6,10(14)-diene was only identified after expression of the *F. mangiferae STC5* gene in *E. coli* (Studt et al., 2016).

Similarly, based on *in vitro* expression of the STC1 TPS and comparison with various plant-derived standards, the *F. fujikuroi STC1* BGC may produce (-)-germacrene D (Niehaus et al., 2017), a compound that may be processed and linearized to the sesquiterpenes we detected. In *F. graminearum kmt6*, all three genes of the homologous *STC1* BGC are co-regulated and more highly expressed than in WT but the lack of nearby co-regulated cytochrome P450 genes makes it less likely that terpenes produced by Stc1 are directly processed into the sesquiterpenes we detected (Fig. 5D). Considering that the sesquiterpenes detected in our *fus1 kmt6* mutant were absent in the two strains in which transcription factors near *STC5* were deleted, we suggest that *F. graminearum* Stc5 is required for the production of tricinolone, tricinolonic acid, tricindiol, and tricinonoic acid.

3.8. Outlook

Our studies with *kmt6* are not complete – more chemistry awaits discovery. Especially promising will be studies that combine partially disabled repressor proteins, for example Kmt6 with slightly altered catalytic function, which result in activation of only a few clusters (Josephson, Connolly, Smith, and Freitag, in preparation). What sets Kmt6 apart from other chromatin modification enzymes that have been eliminated by genetics is its function as a global repressor – deletion results in immediate upregulation of numerous genes, including 78% of all BGCs (see Table 1). Other histone or protein methyltransferases that

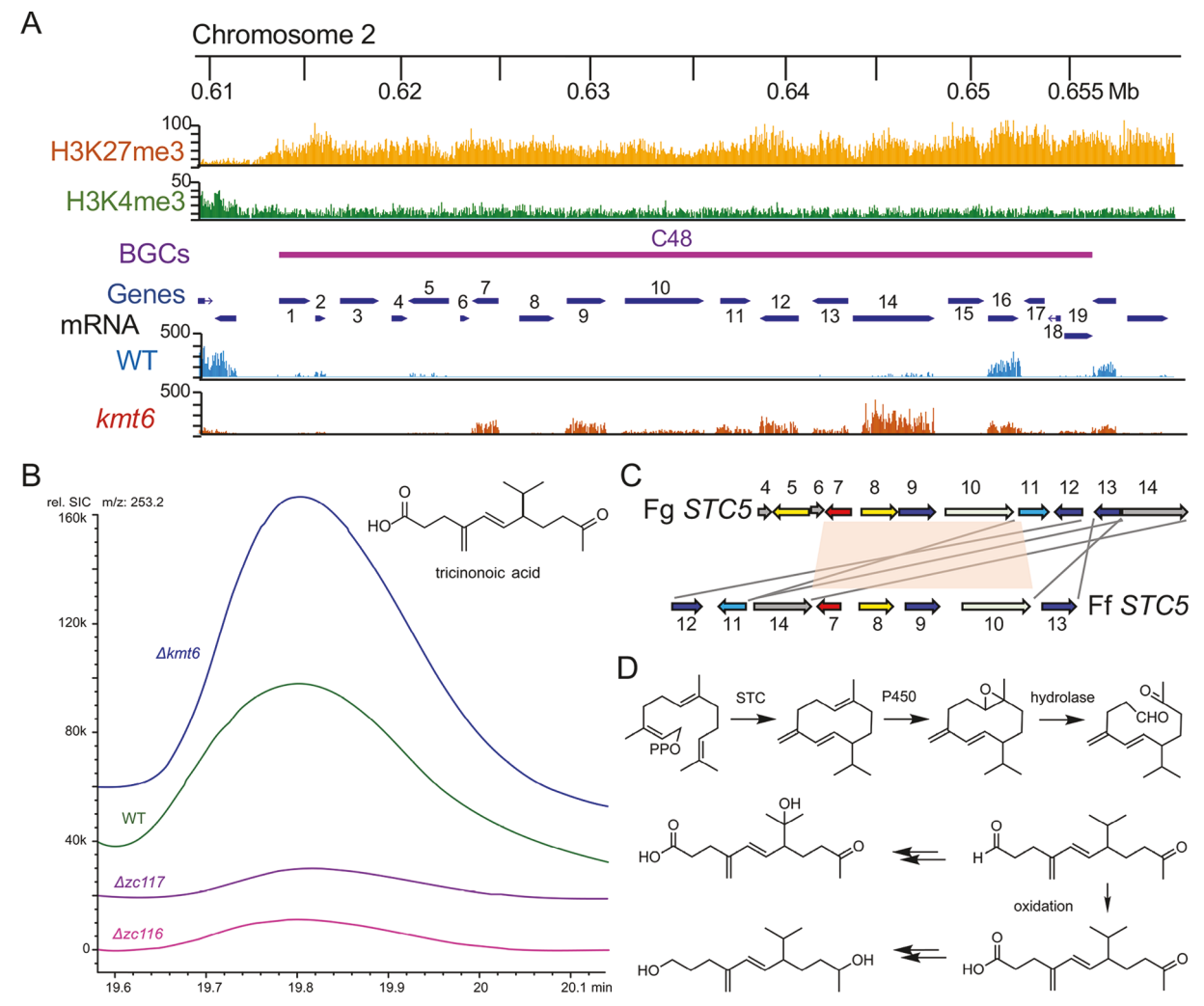


Fig. 5. BGC 48 of *F. graminearum* includes *STC5* and two transcription factor genes, *ZC116*, *ZC117*, involved in the production of tricinonoic acid. (A) Chromatin environment, genes, and RNA-seq of WT and Δkmt6 for C48 (see legend for Fig. 1). Genes in C48: 1, FGSG_08175, conserved hypothetical protein (CHP); 2, FGSG_8176, CHP; 3, FGSG_08177, related to MFS sugar transporter; 4, FGSG_08178, related to acetoacetate decarboxylase; 5, FGSG_08179, *ZC117*; 6, FGSG_08180, CHP; 7, FGSG_08181, related to presilphiperfolan-8-beta-ol synthase (*STC5*); 8, FGSG_08182, *ZC116*; 9, FGSG_08183, predicted cytochrome P450; 10, FGSG_08184, related to nonribosomal peptide synthetase, MxcG-type; 11, FGSG_08185, ABC transporter related to spore wall maturation protein (DIT1), 12, FGSG_08186, predicted cytochrome P450; 13, FGSG_08187, predicted cytochrome P450; 14, FGSG_08188, related to copper-transporting ATPase 2, 15, FGSG_13429, related to integral membrane protein, 16, FGSG_13428, CHP, 17, FGSG_08190, CHP; 18, FGSG_08188, related to trichodiene synthase; 19, FGSG_08191, related to 7-alpha-hydroxycholest-4-en-3-one 12-alpha-hydroxylase. (B) LCMS analysis of WT and Δxc116 and Δxc117 at SIM m/z 253.2 indicating significant reduction of tricinonoic acid production in the transcription factor deletion mutants, but overexpression in Δxc116 and Δxc117 at SIM xc100 are syntenic and conserved, while four additional genes are numbered as in A. Four genes (*STC5*, *ZC116*, a cytochrome P450, and an NRPS-like MxcG-type gene) are syntenic and conserved, while four additional genes are conserved but not syntenic. The eight *F. fujikuroi* genes are regulated by a *ZC116* homolog (Studt et al., 2016), and are also co-ordinately induced in *F. graminearum* Δxc100 but sequentially reduced to yield tricinonoic acid. This can be sequentially reduced to yield tricinolone and tricindiol. Tricinolonoic acid is likely captured directly from the STC enzyme or is oxidized from tricinonoic acid.

have been identified and contribute to transcriptional control of SecMet production, like LaeA or COMPASS (Bok and Keller, 2004; Gerke and Braus, 2014; Soukup et al., 2012) act predominantly as global co-activators, so that absence of these proteins also results in absence of SecMets. Chemical perturbation by inhibitors of histone modification or DNA methylation enzymes have yielded new chemistry (Cherblanc et al., 2013) but the effects are not always predictable or long-lasting, thus using a mutant defective in a global repressor offers benefits for stable metabolite production.

Heterologous expression of biosynthetic gene clusters is improving and has yielded new chemical diversity from natural sources, particularly in the area of fungal natural products discovery (Clevenger et al., 2017; Harvey et al., 2018). While successful about half the time, we believe a combination of our streamlined metabolomics approaches with classic gene activation strategies via

mutation of global repressors, combined with nutrient variation, changes of environmental conditions, application of knowledge of fungal biology, development and chemical ecology will be key to explore the full fungal metabolome holistically and will improve yields of new chemistry. To accelerate the pace of discovery of natural products one corollary is the development of techniques focused on the rapid detection of novel or differentially produced metabolites. Our multivariate analysis enabled the identification and isolation of new and known metabolites from *F. graminaerum* as well as the quantification of the overexpression of SecMets in the *kmt6* mutant. LCMS based metabolomics is well positioned to examine chemical differences between extracts from small scale fungal cultures and helps to prioritize conditions to quickly isolate sufficient amounts of metabolites for full chemical analysis by extensive NMR spectroscopic methods.

Acknowledgements

We acknowledge the support of the Oregon State University NMR Facility funded in part by the National Institutes of Health, HEI Grant 1S10OD018518, and by the M. J. Murdock Charitable Trust grant #2014162. We thank Yin-Won Lee and Hokyoung Son (Seoul National University, Korea) and Frances Trail (Michigan State University) for supplying strains. Research on Kmt6 is funded by NSF grants (MCB1515998, MCB1818006) to MF. Research in the Loesgen Lab is funded by an NSF grant (CH1808717) to SL. Donovon Adpressa acknowledges support from the Department of Chemistry at OSU and support from OSU's Molecular and Cellular Biology Program's Collaboration Catalyzer Award. Zachary Konkel acknowledges support from the Oregon Community Foundation.

Appendix A. Supplementary material

Supplementary data to this article can be found online at https://doi.org/10.1016/j.fgb.2019.103256.

References

- Abdelmohsen, U., et al., 2014. Dereplication strategies for targeted isolation of new antitrypanosomal actinosporins A and B from a marine sponge associated-actinokineospora sp. EG49. Mar. Drugs 12, 1220.
- Abraham, W.-R., Arfmann, H.-A., 1988. Fusalanipyrone, a monoterpenoid from Fusarium solani. Phytochemistry 27, 3310–3311.
- Abraham, W.-R., et al., 1990. Biosynthesis of the terpenoidic polyketide fusalanipyrone*. Phytochemistry 29, 2877–2878.
- Adpressa, D.A., Loesgen, S., 2016. Bioprospecting chemical diversity and bioactivity in a marine derived Aspergillus terreus. Chem. Biodivers. 13, 253–259.
- Adpressa, D.A., et al., 2017. Unexpected biotransformation of the HDAC inhibitor vorinostat yields aniline-containing fungal metabolites. ACS Chem. Biol.
- Aghcheh, R.K., Kubicek, C.P., 2015. Epigenetics as an emerging tool for improvement of fungal strains used in biotechnology. Appl. Microbiol. Biotechnol. 99, 6167–6181.
- Albright, J.C., et al., 2015. Large-scale metabolomics reveals a complex response of Aspergillus nidulans to epigenetic perturbation. ACS Chem. Biol. 10, 1535–1541.
- Bahadoor, A., et al., 2018. Gramillin A and B: Cyclic Lipopeptides Identified as the Nonribosomal Biosynthetic Products of Fusarium graminearum. Journal of the American Chemical Society 140, 16783–16791. https://doi.org/10.1021/jacs. 8b10017.
- Bashyal, B.P., Leslie Gunatilaka, A.A., 2010. Tricinonoic acid and tricindiol, two new irregular sesquiterpenes from an endophytic strain of Fusarium tricinctum. Nat. Prod. Res. 24, 349–356.
- Bian, G., et al., 2018. Metabolic engineering-based rapid characterization of a sesquiterpene cyclase and the skeletons of Fusariumdiene and Fusagramineol from Fusarium graminearum. Org. Lett. 20, 1626–1629.
- Blin, K., et al., 2019. antiSMASH 5.0: updates to the secondary metabolite genome mining pipeline. Nucleic Acids Res. 47, W81–W87.
- Bok, J.W., Keller, N.P., 2004. LaeA, a regulator of secondary metabolism in Aspergillus spp. Eukaryot. Cell 3, 527–535.
- Brakhage, A.A., 2013. Regulation of fungal secondary metabolism. Nat. Rev. Microbiol. 11, 21–32.
- Brakhage, A.A., Schroeckh, V., 2011. Fungal secondary metabolites strategies to activate silent gene clusters. Fungal Genet. Biol. $48,\,15-22.$
- Brown, D.W., et al., 2012. Phylogenomic and functional domain analysis of polyketide synthases in Fusarium. Fungal Biol. 116, 318–331.
- Brown, D.W., Proctor, R.H., 2016. Insights into natural products biosynthesis from analysis of 490 polyketide synthases from Fusarium. Fungal Genet. Biol. 89, 37–51.
- Calvo, A.M., et al., 2002. Relationship between secondary metabolism and fungal development. Microbiol. Mol. Biol. Rev. 66, 447–459.
- Cappellini, R.A., Peterson, J.L., 1965. Macroconidium formation in submerged cultures by a non-sporulating strain of *Gibberella zeae*. Mycologia 57, 962–966.
- Cherblanc, F.L., et al., 2013. Perspectives on natural product epigenetic modulators in chemical biology and medicine. Nat. Prod. Rep. 30, 605–624.Chiang, Y.M., et al., 2009. A gene cluster containing two fungal polyketide synthases
- encodes the biosynthetic pathway for a polyketide, asperfuranone, in Aspergillus nidulans. J. Am. Chem. Soc. 131, 2965–2970.

 Chiara M. et al. 2015. Genome sequencing of multiple isolates highlights subtelomeric
- Chiara, M., et al., 2015. Genome sequencing of multiple isolates highlights subtelomeric genomic diversity within Fusarium fujikuroi. Genome Biol. Evol. 7, 3062–3069.
- Clevenger, K.D., et al., 2017. A scalable platform to identify fungal secondary metabolites and their gene clusters. Nat. Chem. Biol. 13, 895.
- Connolly, L.R., et al., 2018. Application of the Cre/lox system to construct auxotrophic markers for quantitative genetic analyses in Fusarium graminearum. Methods Mol. Biol. 1848, 235–263.
- Connolly, L.R., et al., 2013. The Fusarium graminearum histone H3 K27 methyltransferase KMT6 regulates development and expression of secondary metabolite gene clusters. PLoS Genet. 9, e1003916.
- Cordier, C., et al., 1990. Structures of zearalenone and zearalanone in solution: A high-

- field NMR and molecular modelling study. Magn. Reson. Chem. 28, 835-845.
- Fox, E.M., Howlett, B.J., 2008. Secondary metabolism: regulation and role in fungal biology. Curr. Opin. Microbiol. 11, 481–487.
- Frandsen, R.J., et al., 2016. Black perithecial pigmentation in Fusarium species is due to the accumulation of 5-deoxybostrycoidin-based melanin. Sci. Rep. 6, 26206.
- Gaffoor, I., et al., 2005. Functional analysis of the polyketide synthase genes in the filamentous fungus Gibberella zeae (anamorph Fusarium graminearum). Eukaryot. Cell 4, 1926–1933.
- Gaffoor, I., Trail, F., 2006. Characterization of two polyketide synthase genes involved in zearalenone biosynthesis in Gibberella zeae. Appl. Environ. Microbiol. 72, 1793–1799.
- Gardiner, D.M., et al., 2014. Genome Sequence of Fusarium graminearum Isolate CS3005. Genome Announc. 2.
- Gerke, J., Braus, G.H., 2014. Manipulation of fungal development as source of novel secondary metabolites for biotechnology. Appl. Microbiol. Biotechnol. 98, 8443–8455
- Hansen, F.T., et al., 2015. An update to polyketide synthase and non-ribosomal synthetase genes and nomenclature in Fusarium. Fungal Genet. Biol. 75, 20–29.
- Harris, L.J., et al., 2007. A novel gene cluster in Fusarium graminearum contains a gene that contributes to butenolide synthesis. Fungal Genet. Biol. 44, 293–306.
- Harvey, C.J.B., et al., 2018. HEx: A heterologous expression platform for the discovery of fungal natural products. Sci. Adv. 4.
- $\label{eq:Hegge, A., et al., 2015. Factors influencing production of fusaristatin A in Fusarium graminearum. Metabolites 5, 184.$
- Henke, M.T., et al., 2016. New Aspercryptins, lipopeptide natural products, revealed by HDAC inhibition in Aspergillus nidulans. ACS Chem. Biol. 11, 2117–2123.
- Hou, Y., et al., 2012. Microbial strain prioritization using metabolomics tools for the discovery of natural products. Anal. Chem. 84, 4277–4283.
- Jamieson, K., et al., 2013. Regional control of histone H3 lysine 27 methylation in Neurospora. Proc. Natl. Acad. Sci. USA 110, 6027–6032.
- Janevska, S., et al., 2016. Gibepyrone Biosynthesis in the Rice Pathogen Fusarium fujikuroi Is Facilitated by a Small Polyketide Synthase Gene Cluster. J. Biol. Chem. 291, 27403–27420.
- Jeon, J., et al., 2015. Genome-wide profiling of DNA methylation provides insights into epigenetic regulation of fungal development in a plant pathogenic fungus, Magnaporthe oryzae. Sci. Reports 5, 8567.
- Jia, L.J., et al., 2019. A linear nonribosomal octapeptide from Fusarium graminearum facilitates cell-to-cell invasion of wheat. Nat. Commun. 10, 922.
- Jin, J.M., et al., 2010. Characterization of carotenoid biosynthetic genes in the ascomycete Gibberella zeae. FEMS Microbiol. Lett. 302, 197–202.
- Jorgensen, S.H., et al., 2014. Fusarium graminearum PKS14 is involved in orsellinic acid and orcinol synthesis. Fungal Genet. Biol. 70, 24–31.
- Khaldi, N., et al., 2010. SMURF: Genomic mapping of fungal secondary metabolite clusters. Fungal Genet. Biol. 47, 736-741.
- Kim, Y.T., et al., 2005. Two different polyketide synthase genes are required for synthesis of zearalenone in Gibberella zeae. Mol. Microbiol. 58, 1102–1113.
- Kleigrewe, K., et al., 2012. Structure elucidation of new Fusarins revealing insights in the rearrangement mechanisms of the Fusarium Mycotoxin Fusarin C. J. Agric. Food. Chem. 60, 5497–5505.
- Kroken, S., et al., 2003. Phylogenomic analysis of type I polyketide synthase genes in pathogenic and saprobic ascomycetes. Proc. Natl. Acad. Sci. U S A. 100, 15670–15675.
- Li, L.Y., et al., 2008. Pyrrole and indole alkaloids from an endophytic Fusarium incarnatum (HKI00504) isolated from the mangrove plant Aegiceras corniculatum. J. Asian Nat. Prod. Res. 10, 775–780.
- Lopez-Gallego, F., et al., 2010. Selectivity of fungal sesquiterpene synthases: role of the active site's H-1 alpha loop in catalysis. Appl. Environ. Microbiol. 76, 7723–7733.
- Malz, S., et al., 2005. Identification of a gene cluster responsible for the biosynthesis of aurofusarin in the Fusarium graminearum species complex. Fungal Genet. Biol. 42, 420–433
- Margueron, R., Reinberg, D., 2011. The Polycomb complex PRC2 and its mark in life. Nature 469, 343-349.
- McCormick, S.P., et al., 2010. CLM1 of Fusarium graminearum encodes a longiborneol synthase required for culmorin production. Appl. Environ. Microbiol. 76, 136–141.
- Niehaus, E.-M., et al., 2013. Genetic manipulation of the *Fusarium fujikuroi* fusarin gene cluster yields insight into the complex regulation and fusarin biosynthetic pathway. Chem. Biol. 20, 1055–1066.
- Niehaus, E.M., et al., 2017. The GATA-Type Transcription Factor Csm1 Regulates Conidiation and Secondary Metabolism in Fusarium fujikuroi. Front. Microbiol. 8, 1175.
- Nielsen, K.F., et al., 2011. Dereplication of Microbial Natural Products by LC-DAD-TOFMS. J. Nat. Prod. 74, 2338–2348.
- Oide, S., et al., 2014. Individual and combined roles of malonichrome, ferricrocin, and TAFC siderophores in Fusarium graminearum pathogenic and sexual development. Front. Microbiol. 5, 759.
- Oide, S., et al., 2006. NPS6, encoding a nonribosomal peptide synthetase involved in siderophore-mediated iron metabolism, is a conserved virulence determinant of plant pathogenic ascomycetes. Plant Cell 18, 2836–2853.
- Pluskal, T., et al., 2010. MZmine 2: modular framework for processing, visualizing, and analyzing mass spectrometry-based molecular profile data. BMC Bioinf. 11, 395.
- Proctor, R.H., et al., 1995. Reduced virulence of Gibberella zeae caused by disruption of a trichothecene toxin biosynthetic gene. Mol. Plant Microbe Interact. 8, 593–601.
- Reinoso, R., et al., 2013. Biological activity of macromycetes isolated from chilean subantarctic ecosystems. J. Chil. Chem. Soc. 58, 2016–2019.
- Sarikaya-Bayram, Ö., et al., 2014. Membrane-Bound Methyltransferase Complex VapA-VipC-VapB Guides Epigenetic Control of Fungal Development. Dev. Cell 29, 406–420.

- Schmidt-Dannert, C., 2015. Biosynthesis of terpenoid natural products in fungi. Adv. Biochem. Eng. Biotechnol. 148, 19–61.
- Shaver, S., et al., 2010. Origin of the polycomb repressive complex 2 and gene silencing by an E(z) homolog in the unicellular alga Chlamydomonas. Epigenetics 5, 301–312.
- Shiono, Y., et al., 2007. Fusaristatins A and B, Two New Cyclic Lipopeptides from an Endophytic Fusarium sp. J. Antibiot. 60, 309–316.
- Sieber, C.M.K., et al., 2014. The Fusarium graminearum genome reveals more secondary metabolite gene clusters and hints of horizontal gene transfer. PLoS ONE 9, e110311.
- Smith, K.M., et al., 2008. The fungus Neurospora crassa displays telomeric silencing mediated by multiple sirtuins and by methylation of histone H3 lysine 9. Epigenet. Chromatin 1. 5.
- Son, H., et al., 2011. A phenome-based functional analysis of transcription factors in the cereal head blight fungus, Fusarium graminearum. PLoS Pathog. 7, e1002310.
- Sorensen, J.L., et al., 2012. Production of novel fusarielins by ectopic activation of the polyketide synthase 9 cluster in Fusarium graminearum. Environ. Microbiol. 14, 1159–1170.
- Sørensen, J.L., et al., 2014. Identification of the Biosynthetic Gene Clusters for the Lipopeptides Fusaristatin A and W493 B in Fusarium graminearum and F. pseudograminearum. J. Nat. Prod. 77, 2619–2625.
- Soukup, A.A., et al., 2012. Overexpression of the Aspergillus nidulans histone 4 acetyl-transferase EsaA increases activation of secondary metabolite production. Mol. Microbiol. 86, 314–330.
- Studt, L., et al., 2016. Knock-down of the methyltransferase Kmt6 relieves H3K27me3 and results in induction of cryptic and otherwise silent secondary metabolite gene clusters in Fusarium fujikuroi. Environ. Microbiol. 18, 4037–4054.

- Tobiasen, C., et al., 2007. Nonribosomal peptide synthetase (NPS) genes in Fusarium graminearum, F. culmorum and F. pseudograminearium and identification of NPS2 as the producer of ferricrocin. Curr. Genet. 51, 43–58.
- Trisuwan, K., et al., 2013. Pyrone derivatives from the soil fungus Fusarium solani PSU-RSPG37. Phytochem. Lett. 6, 495–497.
- Vogt, E., Künzler, M., 2019. Discovery of novel fungal RiPP biosynthetic pathways and their application for the development of peptide therapeutics. Appl. Microbiol. Biotechnol. 103, 5567–5581.
- Weber, T., et al., 2015. antiSMASH 3.0—a comprehensive resource for the genome mining of biosynthetic gene clusters. Nucleic Acids Res. 43, W237–W243.
- Westphal, K.R., et al., 2018. Who Needs Neighbors? PKS8 Is a Stand-Alone Gene in Fusarium graminearum Responsible for Production of Gibepyrones and Prolipyrone B. Molecules 23.
- Wiemann, P., et al., 2013. Deciphering the cryptic genome: genome-wide analyses of the rice pathogen Fusarium fujikuroi reveal complex regulation of secondary metabolism and novel metabolites. PLoS Pathog. 9, e1003475.
- Williams, R.B., et al., 2008. Epigenetic remodeling of the fungal secondary metabolome. Org. Biomol. Chem. 6, 1895–1897.
- Wollenberg, R.D., et al., 2017. Chrysogine Biosynthesis Is Mediated by a Two-Module Nonribosomal Peptide Synthetase. Journal of Natural Products 80, 2131–2135. https://doi.org/10.1021/acs.jnatprod.6b00822.
- Wu, H.-H., et al., 2009. Six compounds from marine fungus Y26–02. J. Asian Nat. Prod. Res. 11, 748–751.
- Zou, X., et al., 2011. Two new imidazolone-containing alkaloids and further metabolites from the ascomycete fungus Tricladium sp. Chem. Biodivers. 8, 1914–1920.